# Hierarchical $CuO_x$-$Co_3O_4$ heterostructure nanowires decorated on 3D porous nitrogen-doped carbon nanofibers as flexible and free-standing anodes for high performance lithium-ion batteries

Huanhui Chen, Jiao He, Yongliang Li*, Shan Luo, Lingna Sun, Xiangzhong Ren*, Libo Deng, Peixin Zhang, Yuan Gao, Jianhong Liu

College of Chemistry and Environmental Engineering, Shenzhen University, Shenzhen, Guangdong 518060, P.R. China

Corresponding author:

Xiangzhong Ren, Email: renxz@szu.edu.cn, Tel/Fax: +86-755-26558134

Yongliang Li, Email: liyli@szu.edu.cn, Tel/Fax: +86-755-26536627

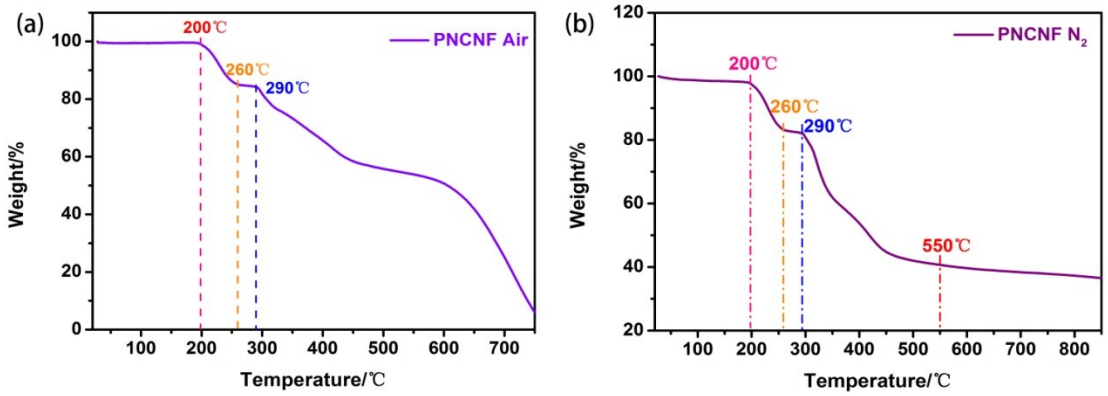


**Fig. S1.** TG curve of PNCNF precursor films under (a) air and (b) $N_2$ atmosphere.

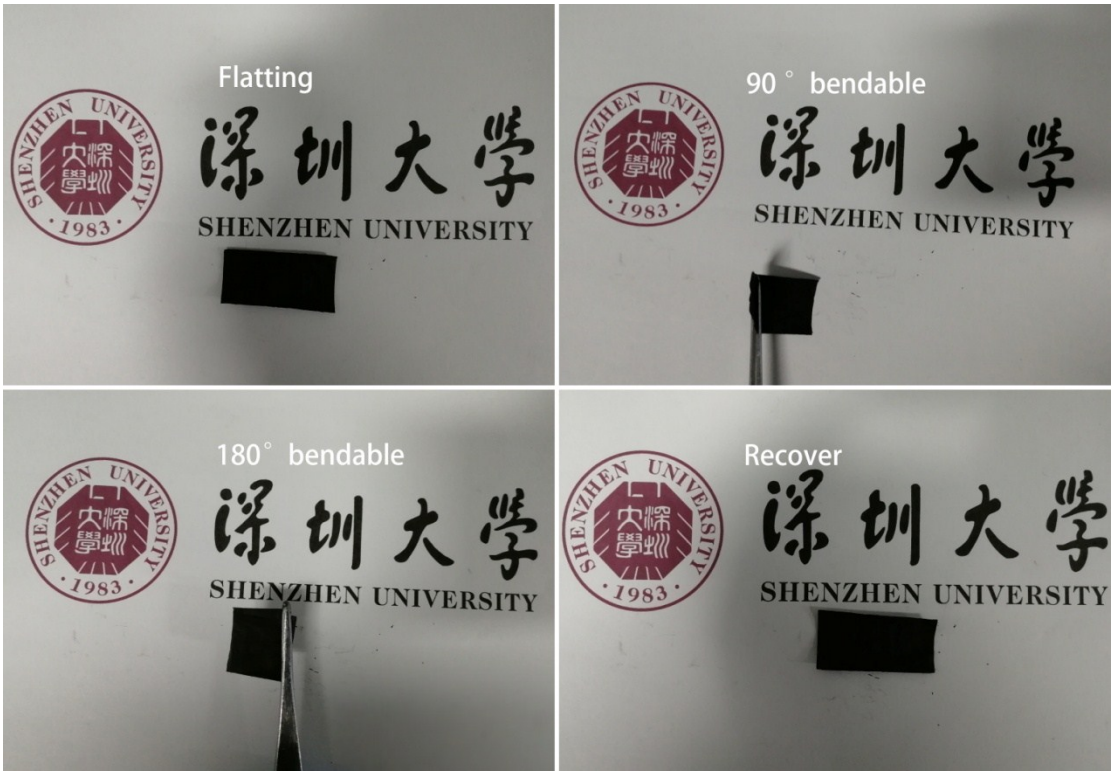


**Fig S2.** Digital images of PNCNF film under flatting, bending (90°, 180°) and recovered states.


**Fig. S3**. Digital image of $CuO_x$-$Co_3O_4$@PNCNF electrode.

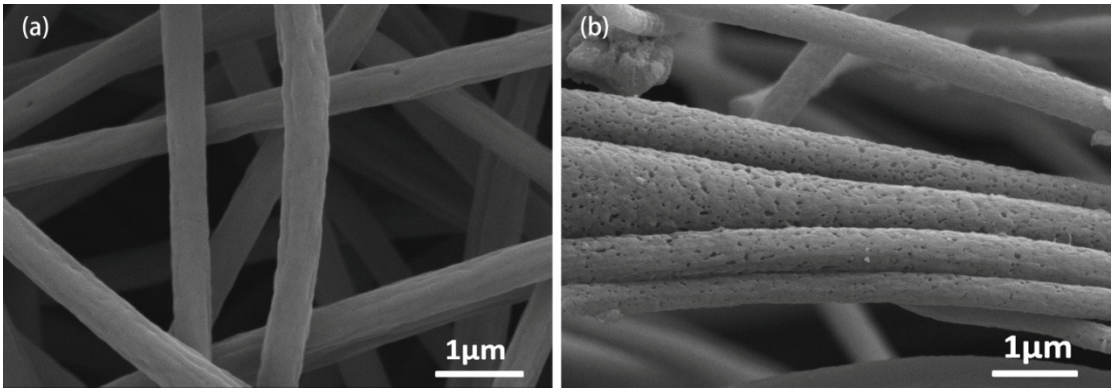


**Fig. S4**. SEM images of the (a) NCNF (without CTAB) and (b) PNCNF (with CTAB) at different magnifications.

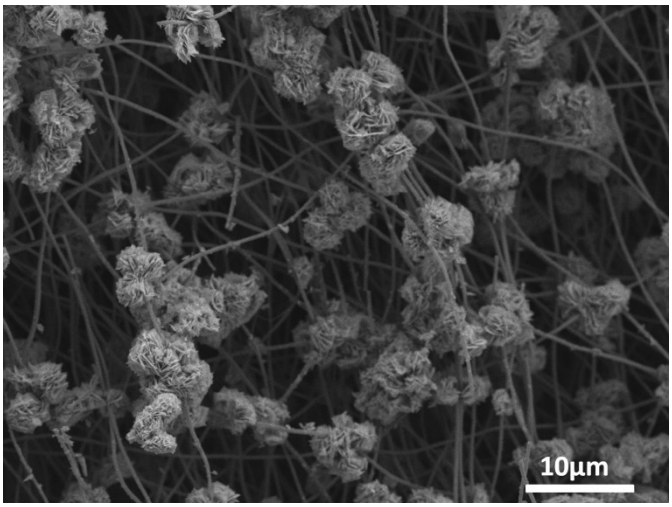


**Fig. S5.** SEM image of $CuO_x$-$Co_3O_4$@NCNF electrode without CTAB.

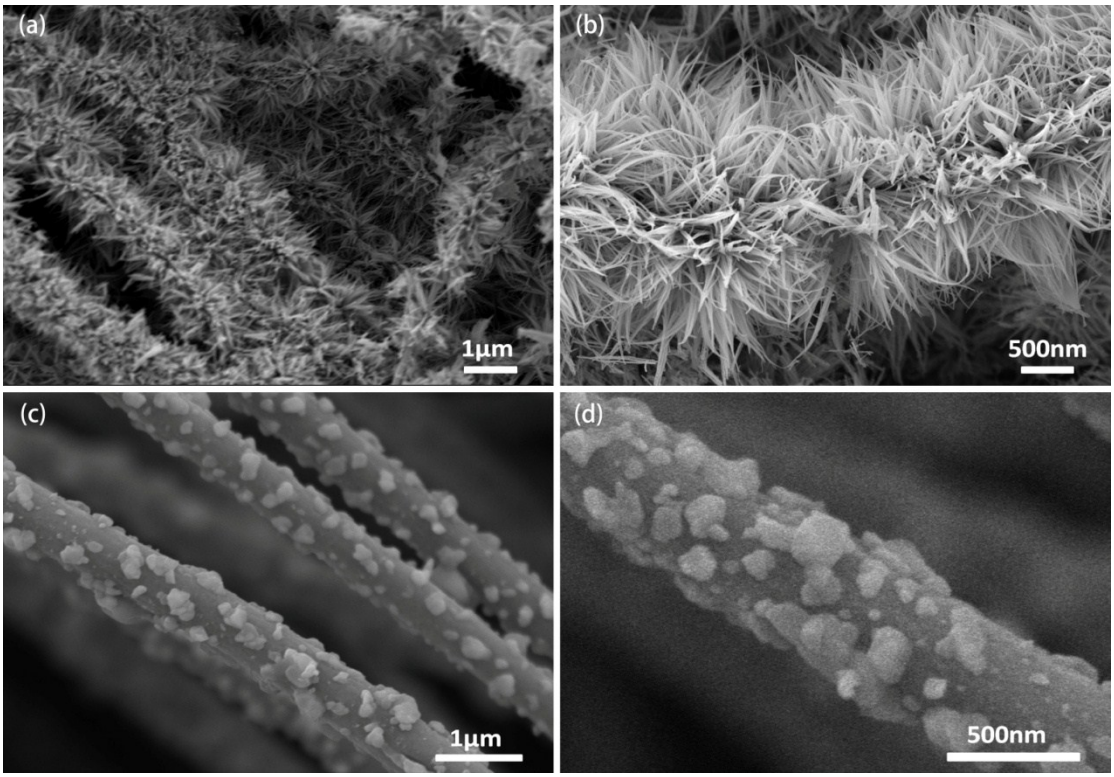


**Fig. S6**. SEM images of the (a and b) $Co_3O_4$@NCNF and (c and d) $CuO_x$@PNCNF at different magnifications.

**Table S1** The elemental composition of $CuO_x$-$Co_3O_4$@PNCNF composite.

| Element | Weight % | Atomic % |
|---|---|---|
| C K | 6.69 | 20.82 |
| N K | 0.96 | 2.56 |
| O K | 10.97 | 25.63 |
| CoK | 63.04 | 40.15 |
| CuK | 18.34 | 10.84 |

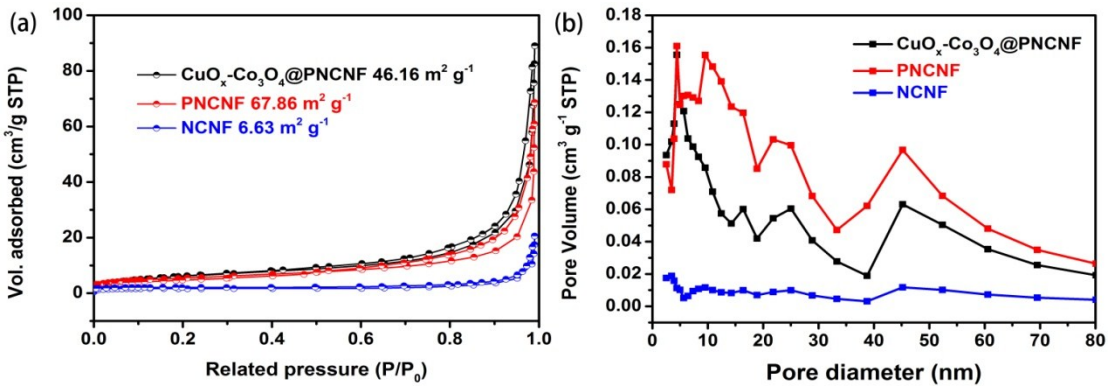


**Fig. S7.** (a) $N_2$ adsorption/desorption isotherms and (b) pore size distributions of NCNF, PNCNF and $CuO_x$-$Co_3O_4$@PNCNF samples.

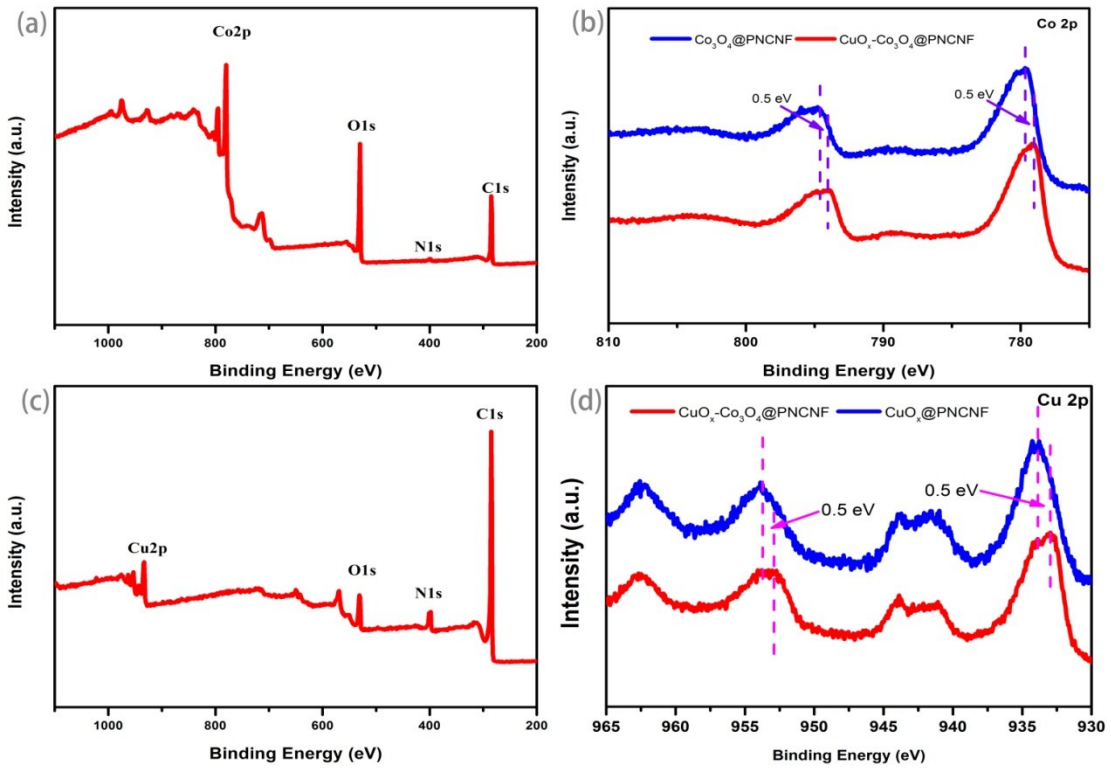


**Fig. S8**. (a) XPS survey scan spectrum for $Co_3O_4$@PNCNF and Core level spectra of (b) Co 2p; (c) XPS full spectrum of $CuO_x$@PNCNF and (d) high-resolution spectra of Cu 2p.

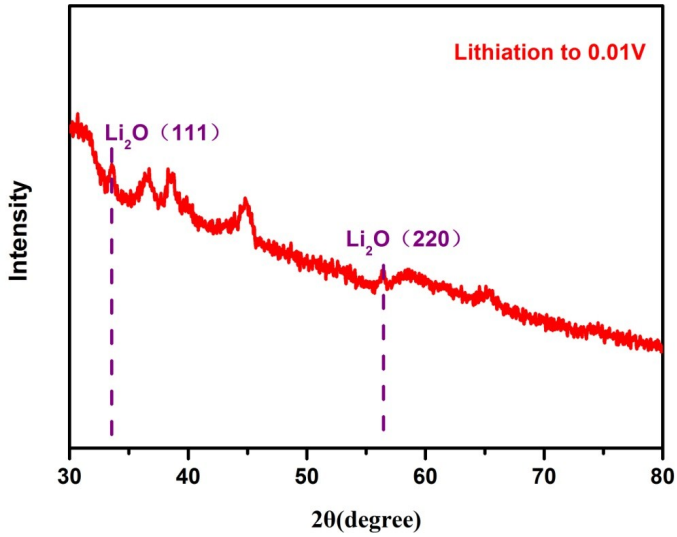


**Fig. S9.** XRD pattern of $CuO_x$-$Co_3O_4$@PNCNF lithiated to 0.01V.

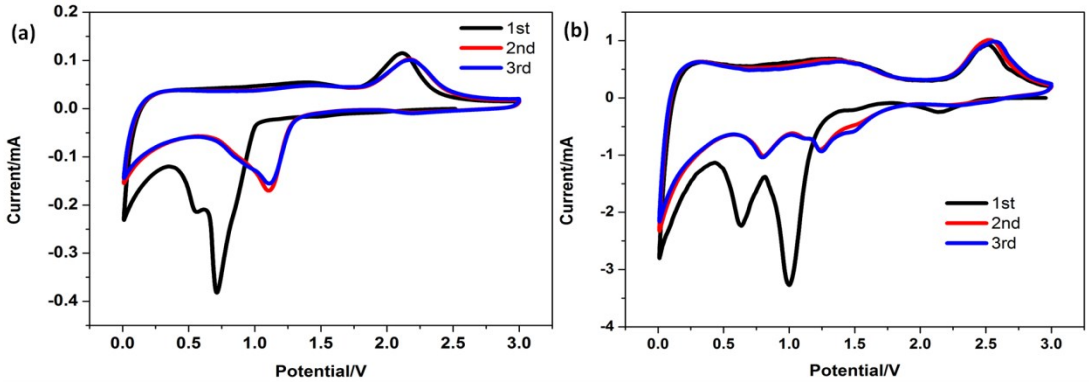


**Fig. S10.** The first three consecutive CV curves of (a) $Co_3O_4$@PNCNF and (b) $CuO_x$@PNCNF.

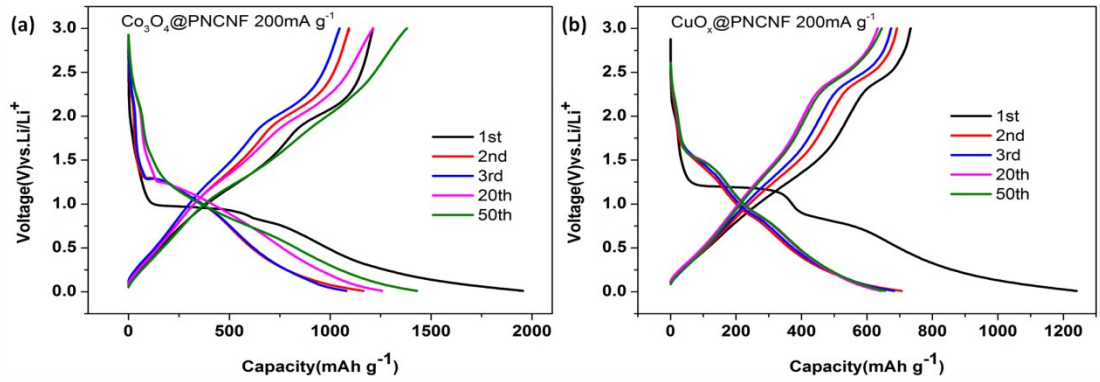


**Fig. S11**. Discharge–charge curves at a current density of 200 mA $g^{-1}$, (a) $Co_3O_4$@PNCNF and (b) $CuO_x$@PNCNF.

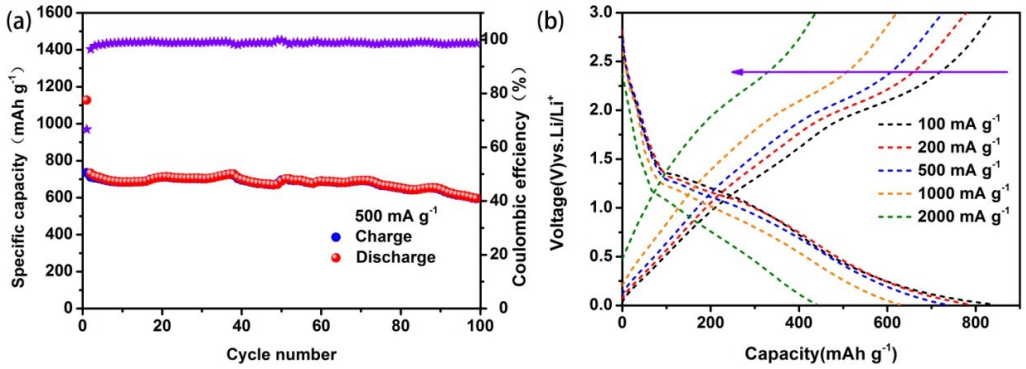


**Fig. S12.** (a) Cycling performance and Coulombic efficiency of $CuO_x$-$Co_3O_4$ electrode at current density of 500 mA $g^{-1}$, (b) Galvanostic charging/discharging curves at various rates of $CuO_x$-$Co_3O_4$ electrode.

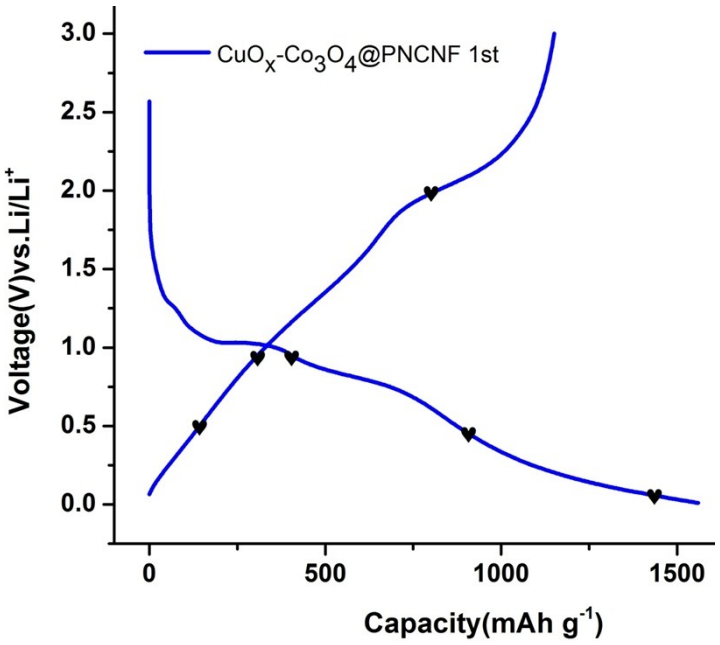


**Fig. S13**.The first cycle at 0.2 A $g^{-1}$ between 0.01 and 3 V.

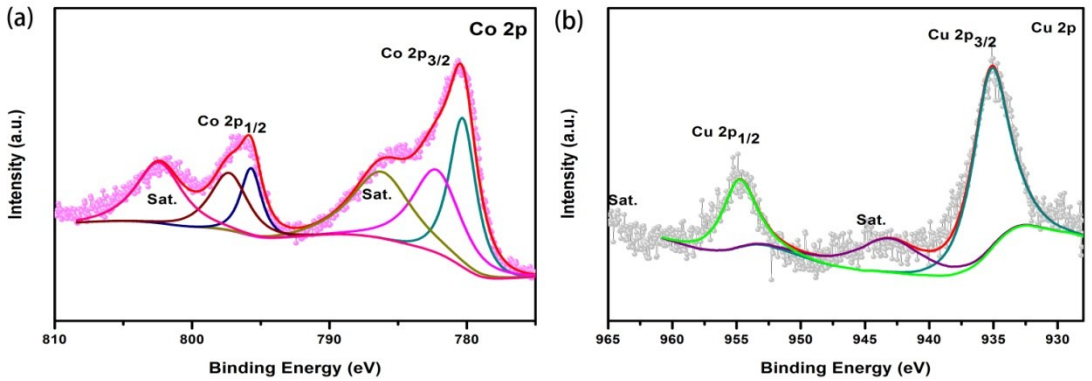


**Fig. S14.** XPS core level spectra of (a) Co 2p and (b) Cu 2p for $CuO_x$-$Co_3O_4$@PNCNF at a current density of 200 mA $g^{-1}$ after 100 cycles.

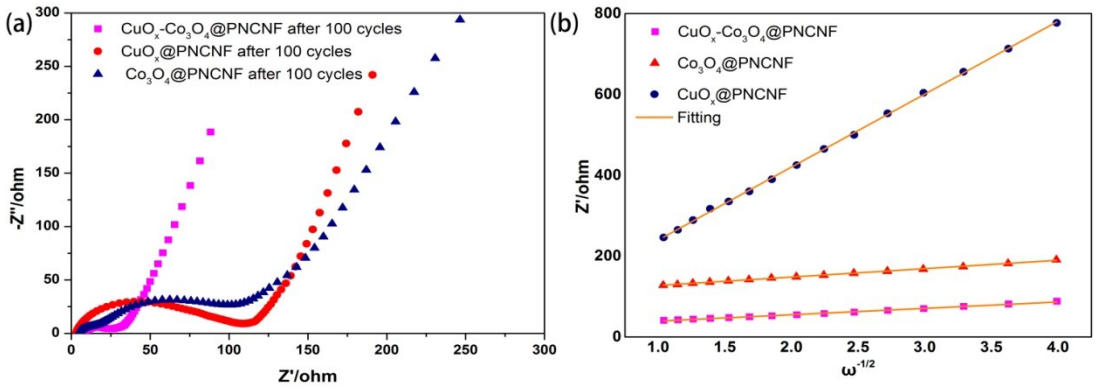


**Fig. S15**. (a) Nyquist plots of three electrodes e after the 100$^{th}$ at 200 mA g$^{-1}$; (b) the corresponding relationships between $Z_{re}$ and $\omega^{-1/2}$ in the frequency region of 0.1–0.01 Hz.

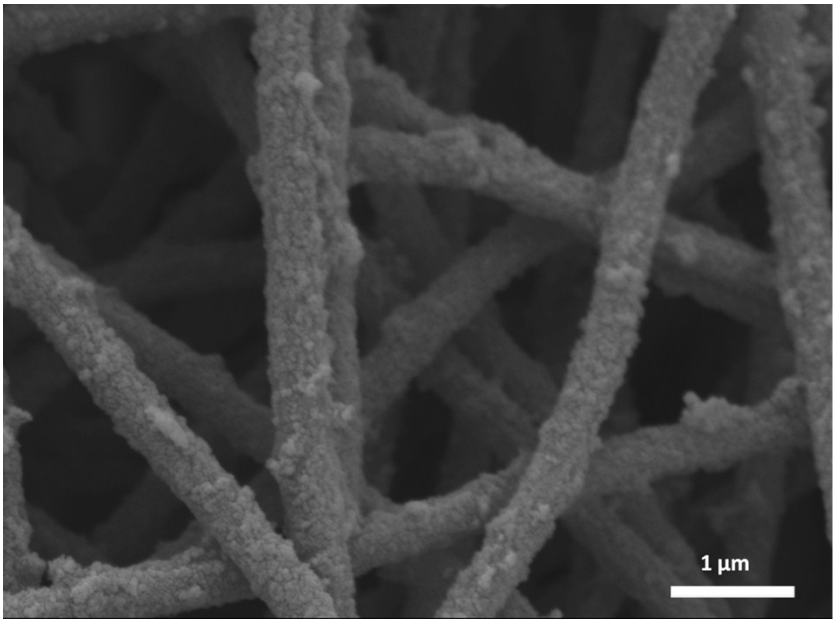


**Fig. S16**. SEM image of $CuO_x$-$Co_3O_4$@PNCNF electrode after the 100$^{th}$ cycle at 200 mA g$^{-1}$.

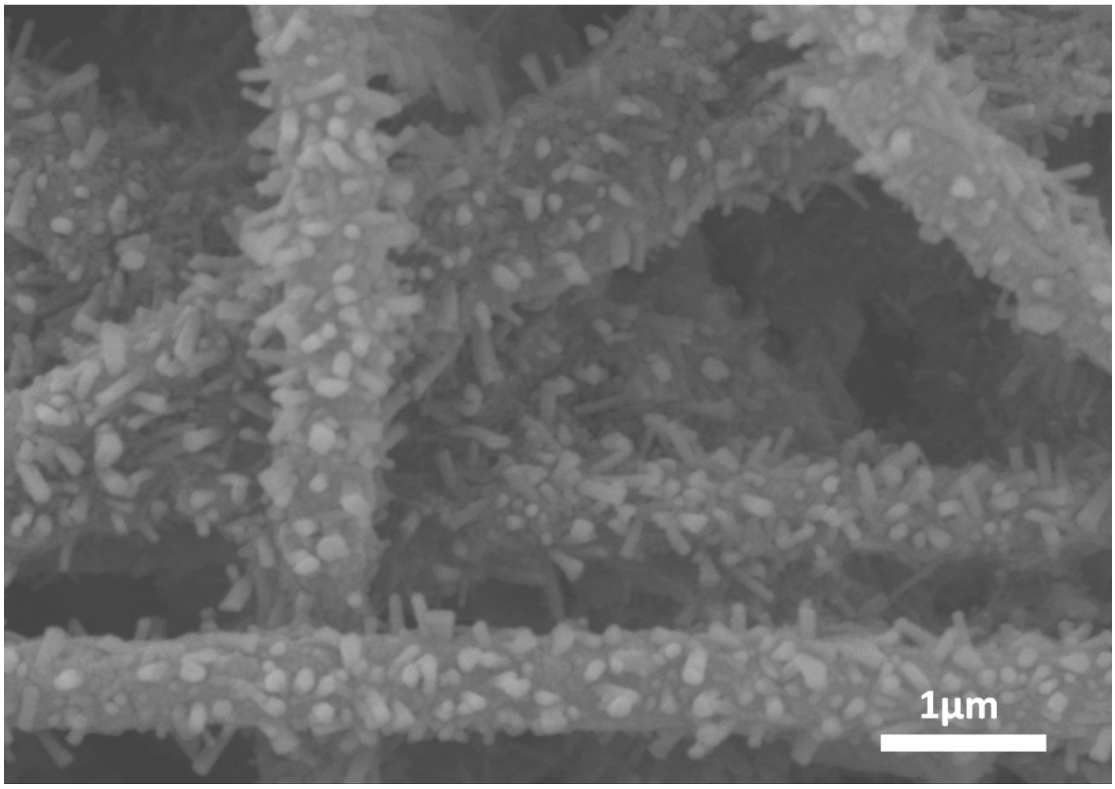


**Fig. S17**. SEM image of $CuO_x$@PNCNF electrode after the 100$^{th}$ cycle at 200 mA g$^{-1}$.

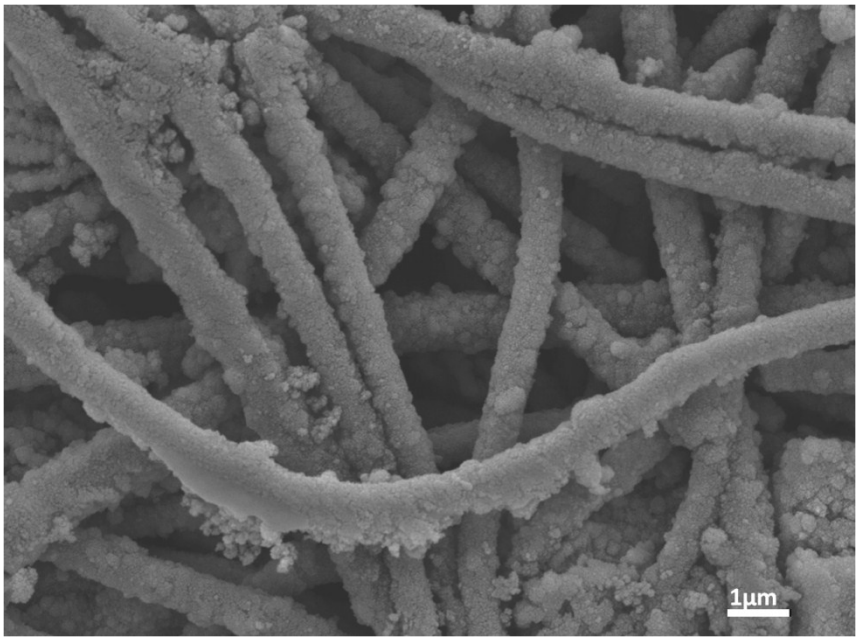


**Fig. S18**. SEM image of $Co_3O_4$@PNCNF electrode after the 100$^{th}$ cycle at 200 mA g$^{-1}$.

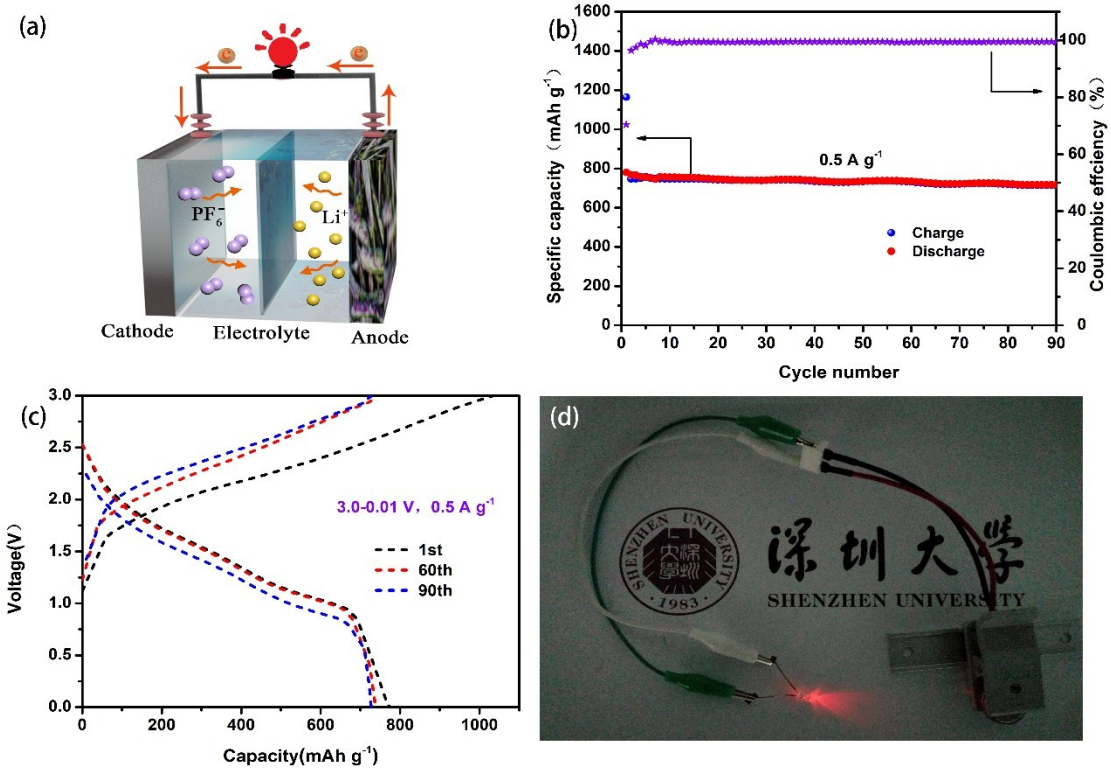


**Fig. S19.** (a) Schematic illustration of the full lithium-ion cell with $CuO_x$-$Co_3O_4$@PNCNF- $LiFePO_4$/Al couple; (b) Charge and discharge curves and (c) cycling performance of the full battery at 0.5 A $g^{-1}$ in the voltage range of 0.01–3.0 V; (d) digital photo of $CuO_x$-$Co_3O_4$@PNCNF- $LiFePO_4$/Al full cells to light red LED.

**Table. S2**. Comparison of the electrochemical lithium storage performance of the $CuO_x$-$Co_3O_4$@PNCNF electrodes presented in this work and reported electrodes in the literature.

| Materials | Reversible capacity ($mAhg^{-1}$)/Cycle number | | | | | Ref. |
|---|---|---|---|---|---|---|
| | Current density 100mA $g^{-1}$ | Current density 200mA $g^{-1}$ | Current density 500mA $g^{-1}$ | Current density 1000mA $g^{-1}$ | Current density 2000mA $g^{-1}$ | |
| CuO@C octahedra | | | 512/300th | | | 1 |
| F-CuO | | | 785/100th | 624/300th | 370/10th | 2 |
| CuO@NiO | 1061/200th | | 523/100th | 376/100th | 193/400th | 3 |
| MWCNTs/$Co_3O_4$ | 813/100th | | | 514/10th | | 4 |
| $Co_3O_4$@$TiO_2$ | | 803/100th | | 400/600th | | 5 |
| $Co_3O_4$/N–C | | 883/130th | | 612/500th | | 6 |
| $Co_3O_4$/$ZnCo_2O_4$ | | | | | 409/500th | 7 |
| $NiCo_2O_4$–C nanorods | 1183/200th | | 863/200th | | 594/200th | 8 |
| CoO@C | | 991/300th | 840/300th | | 587/550th | 9 |
| **$CuO_x$-$Co_3O_4$@PNCNF** | | **1122/100th** | **889/10th** | **812/10th** | **663/1000th** | **This work** |

**Table. S3**. $R_{ct}$, $\sigma$ and $D_{Li+}$ values determined from the EIS for all the electrodes.

| | $R_{ct}$（Ω） | $\sigma$（Ω cm$^2$ s$^{-0.5}$） | $D_{Li+}$（cm$^2$ s$^{-1}$） |
|---|---|---|---|
| **$CuO_x$@PNCNF** | 73.5 | 386.8 | $1.0\times10^{-15}$ |
| **$Co_3O_4$@PNCNF** | 88.9 | 280.2 | $1.9\times10^{-15}$ |
| **$CuO_x$-$Co_3O_4$@PNCNF** | 35.9 | 196.6 | $3.9\times10^{-15}$ |

## References


1. T. Chen, Y. Hu, B. Cheng, Ren. Chen, H. Lv, L. Ma, G. Zhu, Y. Wang, C. Yan, Z. Tie, Z. Jin, J. Liu, *Nano Energy,* 2016, **20**, 305-314.
2. Z. Ma, K. Rui, Q. Zhang, Y. Zhang, M. Du, D. Li, Q. Wang, X. Huang, J. Zhu and W. Huang, *Small*, 2017, **13**, 1603500.
3. W. Guo, W. Sun and Y. Wang, *ACS Nano,* 2015, **9**, 11462-71.
4. Ga. Huang, . Zhang, X. Du, Y. Qin, D Yin, and L. Wang, *ACS Nano*, 2015, **9**, 1592-9.
5. H. Geng, H. Ang, X. Ding, H. Tan, G. Guo, G. Qu, Y. Yang, J. Zheng, Q. Yan and H. Gu, *Nanoscale*,2016, **5**,2967–2973.
6. X. Han, W. Chen, X. Han, Y. Tan, D. Sun, *J. Mater. Chem. A*,2016, **4**,13040–13045.
7. W. Song, K. Ji, A. Aguadero, P. Shearing, D. Brett, F. Xie, D. Jason Riley, *Energy Storage Mater.*, 2018, **14**, 324–334.
8. L. Peng, H. Zhang, Y. Bai, J. Yang, Y. Wang, *J. Mater. Chem. A*,2015, **3**, 22094-22101.
9. F. Wu, S. Zhang, B. Xi, Z. Feng, D. Sun, X. Ma, J. Zhang, J. Feng, S. Xiong, *Adv. Energy Mater.*, 2018, **8**, 1703242.